

Phase structure of uniaxially oriented polyethylene films as studied by high resolution solid state ^{13}C n.m.r. spectroscopy

Masaru Nakagawa, Fumitaka Horii* and Ryozo Kitamaru

Institute for Chemical Research, Kyoto University, Uji, Kyoto 611, Japan

(Received 20 March 1989; accepted 20 April 1989)

High resolution solid state ^{13}C nuclear magnetic resonance (n.m.r.) measurements have been made at room temperature for uniaxially oriented polyethylene films by setting the drawing direction parallel to the static magnetic field. Two sharp lines assignable to the crystalline and non-crystalline components appear at 11.8 and 32.6 ppm, respectively, indicating that this sample contains highly oriented crystalline regions and almost disordered non-crystalline regions. On the basis of ^{13}C spin-spin relaxation time measurements and lineshape analyses, the non-crystalline line can be further resolved into two components, crystalline-amorphous interphase and amorphous component. The thickness of the interfacial component has been estimated to be $\approx 90 \text{ \AA}$ †, which is extraordinarily large compared with the values for the isothermally crystallized polyethylenes and the theoretical value. On the other hand, the crystalline resonance line is found to be composed of three components with different spin-lattice relaxation times. The origin of these components is also briefly discussed.

(Keywords: phase structure; polyethylene; oriented films; non-crystalline structure; interphase; high resolution solid state ^{13}C n.m.r.)

INTRODUCTION

In a previous paper¹ we investigated the solid structure of uniaxially oriented polyethylene films above room temperature by high resolution solid state ^{13}C nuclear magnetic resonance (n.m.r.) spectroscopy. Since the sample was drawn to 600% above the melting temperature and then crystallized at room temperature with the length kept constant, a unique morphological structure was produced²; the molecular chains in the crystallites are highly oriented parallel to the drawing direction, whereas the non-crystalline chains are almost disordered. Therefore, a high resolution resonance line, which is assignable to the crystalline component, can be observed at the chemical shift corresponding to the principal value σ_{33} of the chemical shift tensor, by setting the drawing direction parallel to the static magnetic field without magic angle spinning (MAS). In addition, another high resolution line, which is ascribed to the non-crystalline component, appears somewhat downfield as a result of the average of the chemical shift anisotropy by the enhanced molecular motion of this component. In the previous work¹ we analysed these two lines by measuring ^{13}C spin-lattice relaxation behaviour, but we could not detect the crystalline-amorphous interphase, which is defined as a transition region between the crystalline and completely disordered regions.

More recently we measured ^{13}C spin-spin relaxation behaviour of the non-crystalline component for linear polyethylene samples isothermally crystallized from the melt under a MAS condition at room temperature³. In this case we can discriminate between the interfacial

component and the amorphous component because these components have different ^{13}C spin-spin relaxation times (T_{2C}). On the basis of this result, the ^{13}C total spectra of the samples can be well resolved into the crystalline, interfacial and amorphous contributions, which are described by single Lorentzian functions with different chemical shifts and linewidths. Nevertheless, ^{13}C spin-lattice relaxation times (T_{1C}) are still the same for the two non-crystalline components. This may be due to the difference in frequency for the molecular motions determining T_{1C} and T_{2C} relaxations. In other words, the non-crystalline region seems homogeneous in the higher frequency motion, which is associated with the rather short-range structure of the chains.

In this study we applied almost the same method as for the isotropic polyethylene samples to the uniaxially oriented sample in order to characterize the crystalline, interfacial and amorphous regions of the sample. However, the spectra and the T_{1C} and T_{2C} relaxations have been measured for this sample by setting the drawing direction parallel to the static magnetic field without using magic angle sample spinning.

EXPERIMENTAL

Sample

Uniaxially oriented polyethylene films were prepared as follows². Films of molecular weight fraction ($\bar{M}_v = 3.8 \times 10^5$) were irradiated to 8.5 Mrad with γ -rays from a ^{60}CO source at room temperature in vacuum. After removal of the sol fraction by extraction, the films were uniaxially drawn six times at 160°C and crystallized from the stretched and molten state by cooling at room

* To whom correspondence should be addressed

† $1 \text{ \AA} = 10^{-10} \text{ m}$

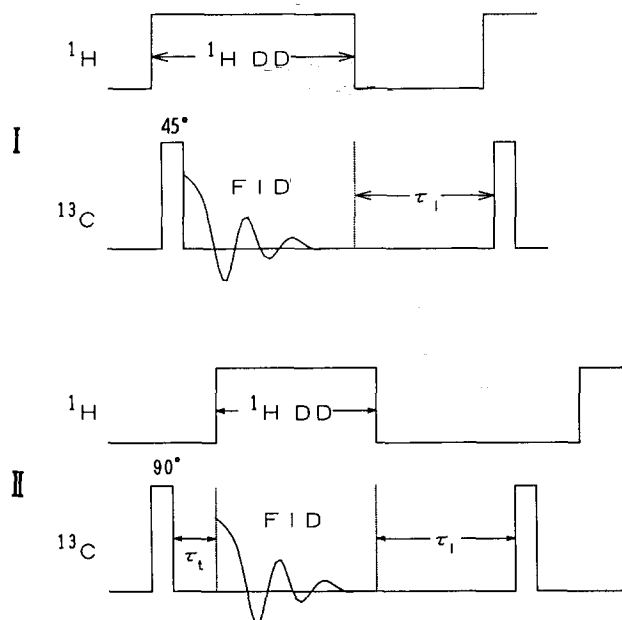


Figure 1 Pulse sequences used in this work

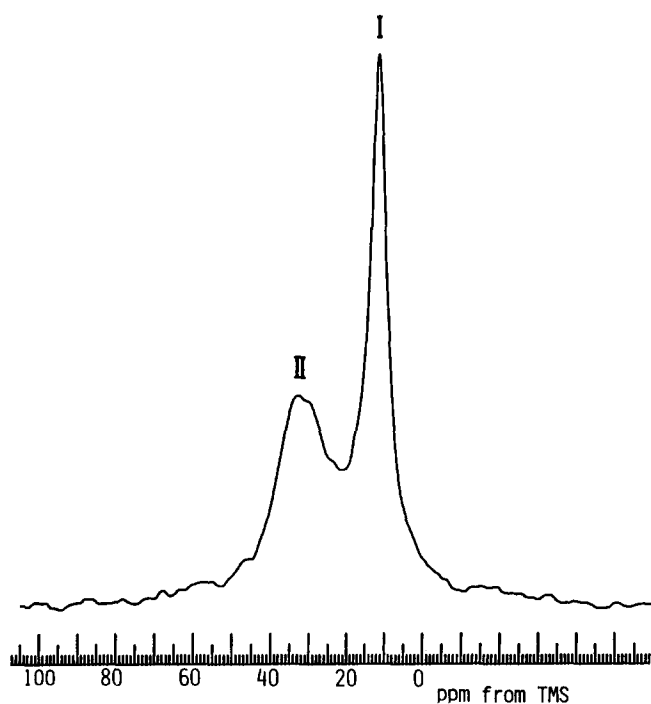


Figure 2 50 MHz DD ^{13}C n.m.r. spectrum of uniaxially oriented polyethylene films obtained by pulse sequence I; drawing direction parallel to B_0

temperature, with the length of the film kept unchanged. The long period of the sample was estimated to be 640 Å by a small angle X-ray scattering method.

^{13}C n.m.r. measurements

50 MHz dipolar-decoupled (DD) ^{13}C n.m.r. measurements were made at room temperature for the uniaxially drawn polyethylene sample with its drawing axis set parallel to the static magnetic field B_0 on a Jeol JNM-FX200 n.m.r. spectrometer operating at 1.4 T. The ^1H and ^{13}C radiofrequency field strengths $\gamma B_1/2\pi$ were 69.4 kHz for the cross polarization (CP) and other pulse sequences used in this work, except for the dipolar decoupling (DD) process, where the ^1H field strength

was reduced to 59.5 kHz. Chemical shifts relative to tetramethylsilane (Me_4Si) were determined by using the CH line at 29.5 ppm of solid adamantane as an external reference.

The pulse sequences used are shown schematically in Figure 1. Pulse sequence I, 45° single pulse sequence, is usually used to obtain ^{13}C n.m.r. spectra instead of the CP technique. When the waiting time τ_1 after the acquisition of FID is set to a larger value than three times the maximum $T_{1\text{C}}$, one can obtain the spectrum quantitatively reflecting the contributions from all components in the sample. Pulse sequence II was used to measure the ^{13}C spin-spin relaxation behaviour under a condition of ^1H non-decoupling. Here, the contribution from a rigid or less mobile component, which has a longer $T_{1\text{C}}$, can be suppressed by setting τ_1 to an appropriate small value. The ^{13}C spin-lattice relaxation process was observed by the pulse sequence with CP developed by Torchia⁴ or by the saturation recovery pulse sequence modified for solid state measurements: $T_{1\text{C}}$ s longer than several tens of seconds were measured by the former pulse sequence, while values shorter than a few seconds were determined by the latter.

RESULTS AND DISCUSSION

Dipolar-decoupled ^{13}C n.m.r. spectrum and ^{13}C spin relaxations

Figure 2 shows the 50 MHz DD ^{13}C n.m.r. spectrum obtained by pulse sequence I for the uniaxially oriented polyethylene films (OPE). Since τ_1 is set to 4500 s, which is three times the longest $T_{1\text{C}}$ for OPE, this spectrum quantitatively reproduces the contributions from all structural components. Two distinct lines, I and II, appear at 11.8 and 32.6 ppm, respectively, relative to Me_4Si . Two similar lines have been observed for a cold drawn polyethylene sample⁵, but line II is more clearly resolved in our sample. The chemical shift of line I is in good accord with the principal value σ_{33} of the chemical shift tensor for polyethylene and n-alkanes with the orthorhombic crystal form⁵⁻⁸. On the other hand, the chemical shift of line II is close to that observed for $\text{n-C}_{17}\text{H}_{36}$ in liquid or polyethylene in solution⁹. Therefore, we simply assign lines I and II to the crystalline and non-crystalline components, respectively. More detailed assignments will be given below.

To determine whether each line consists of a single component, we measured $T_{1\text{C}}$ s by the pulse sequence developed by Torchia⁴ or by the modified saturation-recovery pulse sequence. The $T_{1\text{C}}$ values thus obtained are shown in Table 1 together with the $T_{2\text{C}}$ values described below. Line I exhibits three different $T_{1\text{C}}$ values of 1100, 60.5 and 5.0 s. Three similar components were

Table 1 ^{13}C chemical shifts and spin relaxation times of resonance lines I and II

	Line I	Line II
Chemical shift (ppm)	11.8	32.6
$T_{1\text{C}}$ (s)	1100 60.5 5.0	0.37
$T_{2\text{C}}$ (μs)	—	370 32

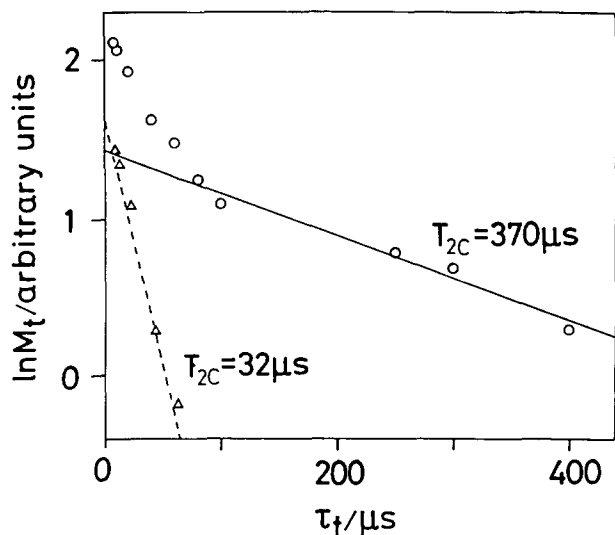


Figure 3 ^{13}C spin-spin relaxation decays for line II, measured by pulse sequence II

observed for the isothermally crystallized polyethylene samples³, which were detected by ^{13}C spin-lattice relaxation under magic angle spinning. The longest T_{1C} component is readily assignable to the rigid crystalline component with a relatively thick lamellar structure. The other two components, however, are not well characterized at present, although both also belong to the crystalline component. A more detailed discussion will be given below.

In contrast to line I, line II consists of a single component with $T_{1C}=0.37\text{ s}$. Such a short T_{1C} suggests the existence of enhanced molecular motion in the non-crystalline region, as also observed for the isothermally crystallized polyethylene samples³. Moreover, the non-crystalline region seems homogeneous in structure on the time scale of 10^{-8} s associated with the T_{1C} relaxation.

In an attempt to discriminate between the amorphous region and the crystalline-amorphous interfacial region, we measured the ^{13}C spin-spin relaxation, which is related to a slower molecular motion than the case of the T_{1C} relaxation. Figure 3 shows the semilogarithmic plot of the peak intensity of line II as a function of τ_t , which was measured by pulse sequence II. In this case the contribution of line I was suppressed by setting $\tau_1=5\text{ s}$. The overall decay curve, which is indicated by open circles in Figure 3, can be resolved into two exponentials by using a least-squares method with a computer. The slower decay yields $T_{2C}=370\ \mu\text{s}$, while the rapid decay gives $T_{2C}=34\ \mu\text{s}$. Two similar components were observed for the bulk crystallized polyethylene sample and the longer and shorter T_{2C} components were assigned to the rubbery and interfacial components, respectively, on the basis of some additional experimental results³. This assignment can also be applied to the present case and other evidence supporting this assignment is given below.

Figure 4 shows the spectrum of the component with $T_{2C}=370\ \mu\text{s}$, which was measured by pulse sequence II by setting $\tau_1=200\ \mu\text{s}$ to suppress the contribution of the interfacial component with $T_{2C}=34\ \mu\text{s}$. This spectrum is obtained by setting the draw axis of the sample parallel to the static magnetic field. Almost the same spectrum is also observed at the same chemical shift (32.6 ppm)

when the draw axis is set perpendicular to the static magnetic field, as shown in Figure 4B. This indicates that the component with $T_{2C}=370\ \mu\text{s}$ undergoes spherically isotropic random motion and can be assigned to the amorphous component in the rubbery state.

Spectral analysis

As shown in the preceding section, there are three components with different T_{1C} values in the crystalline region of OPE, while the non-crystalline region consists of two components, interfacial and amorphous. According to this characterization, we resolve the total spectrum shown in Figure 2 into crystalline, interfacial and amorphous components to estimate their mass fractions. To this end we determine the lineshape for the respective components by using the subtraction method for the spectra.

Figure 5A shows the whole spectrum of the non-crystalline component, which was measured by pulse sequence II by setting $\tau_1=5\text{ s}$ and $\tau_t=0.5\ \mu\text{s}$. Here, an additional small resonance line appearing upfield is part of the crystalline component with $T_{1C}=5.0\text{ s}$. To eliminate this component from the spectrum, we determined the lineshape of the crystalline component, which is shown in Figure 5B, by subtracting the spectrum in Figure 5A from the spectrum measured by pulse sequence II with $\tau_1=8\text{ s}$ and $\tau_t=0.5\ \mu\text{s}$. Figure 5C shows the spectrum reflecting the whole non-crystalline component, obtained by subtracting Figure 5B from Figure 5A. This spectrum has an asymmetric lineshape with upfield tailing, indicating that such asymmetry may stem from the interfacial component. Since the spectrum of the amorphous component (Figure 5D) is obtained by pulse sequence II as a longer T_{2C} component as described above, the spectrum of the interfacial component can be

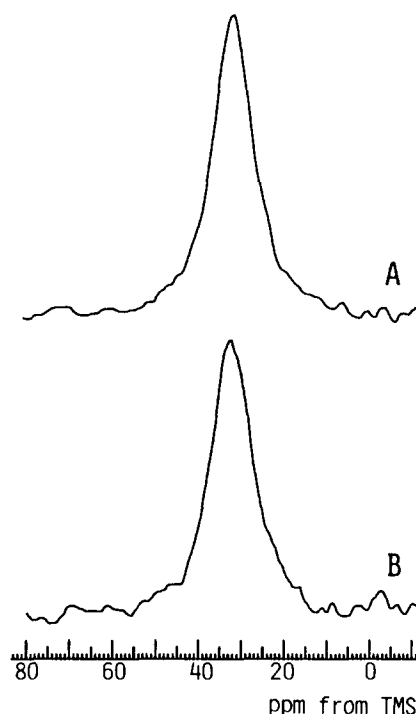


Figure 4 Partially relaxed spectra of the non-crystalline components with $T_{2C}=370\ \mu\text{s}$, measured by pulse sequence II with $\tau_1=5\text{ s}$ and $\tau_t=200\ \mu\text{s}$. A, Drawing direction parallel to B_0 ; B, drawing direction perpendicular to B_0

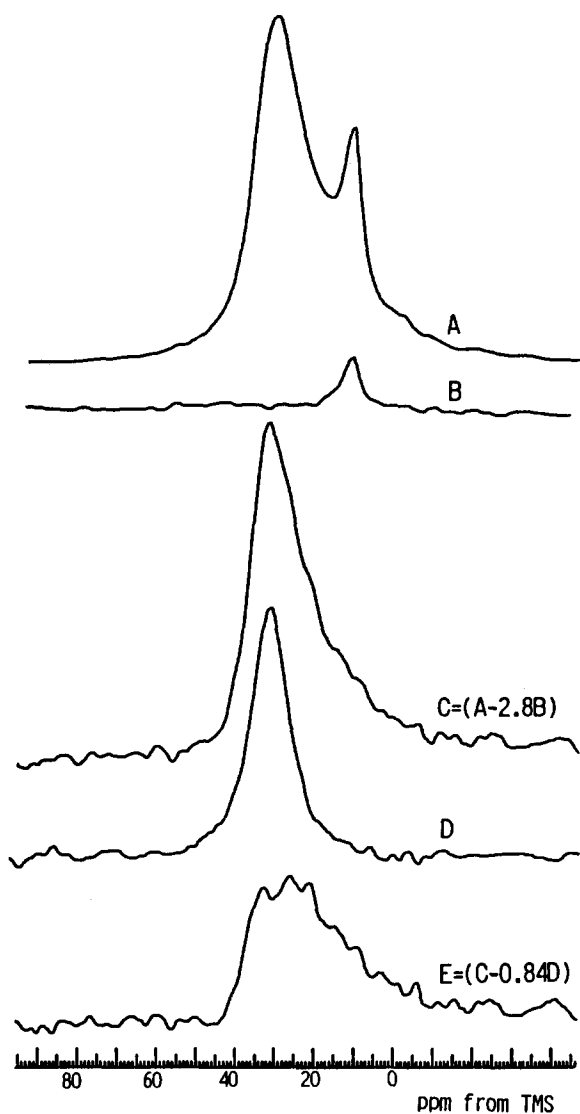


Figure 5 ^{13}C n.m.r. spectra of the respective components: A, non-crystalline component with a small amount of the crystalline component ($T_{1C}=5.0\text{s}$); B, crystalline component ($T_{1C}=5.0\text{s}$); C, non-crystalline component ($(A)-2.8(B)$); D, amorphous component; E, interfacial component ($(C)-0.84(D)$)

obtained by subtracting *Figure 5D* from *Figure 5C*, as shown in *Figure 5E*. As expected, the interfacial component has an asymmetric lineshape with upfield tailing.

Using these lineshapes, the total spectrum of OPE has been resolved into crystalline, interfacial and amorphous components, as shown in *Figure 6*. Here, the crystalline spectrum is separated by subtracting *Figure 5C* from the total spectrum. This component can be well described by a single Lorentzian function, although it has three components with different T_{1C} values. On the other hand, the non-crystalline spectrum can be resolved into interfacial and amorphous components by the spectral subtraction method as mentioned above. As a result, the mass fractions of the crystalline, interfacial and amorphous components are estimated to be 0.50, 0.29 and 0.21, respectively, by calculating the integral intensities of the respective components. The mass fraction of the crystalline component thus obtained is lower than the degree of crystallinity (0.64) determined from density measurements. This disagreement may be due to the overestimation of the latter method, where a

two-phase model consisting of the crystalline and amorphous phases is assumed. In this sample the density of the interfacial region must be considerably increased because of the ordering of the segments in this region. Then the degree of crystallinity should be overestimated as long as the two-phase model is used. In contrast, the density of the interfacial region would be calculated to be 0.921 g cm^{-3} by assuming the three-phase structure shown in *Figure 6*, when the densities of the crystalline and amorphous regions are 1.000 and 0.851 g cm^{-3} , respectively¹⁰.

Phase structure

A separate X-ray small-angle scattering study has revealed that the uniaxially drawn sample used in this work has a lamellar structure with a long period of 640 \AA . On the basis of this result, the thicknesses l_j of the crystalline, interfacial, and amorphous regions are calculated by the following equation:

$$l_j = Lw_j/2 \quad (1)$$

where L is the long period and w_j is the mass fraction of each component. The resultant thicknesses of the crystalline, interfacial and amorphous regions are 320 , 93 and 134 \AA , respectively. The phase structure thus revealed is shown schematically in *Figure 7*.

The thickness of the interfacial component of OPE is much larger than the value (34 \AA) obtained for the isotropic samples isothermally crystallized from the melt³ or the theoretical value ($15\text{--}20\text{ \AA}$) calculated by Flory *et al.*^{11,12} using a lattice model. The cause of such a large disagreement may be related to the difference in crystallization mode. According to the theory of Flory *et al.*^{11,12}, the interfacial region is the transition region between the crystalline and amorphous regions, where the conformation of the segments is still limited because the ends of the segments are connected to the crystallites. In isothermal crystallization from the melt, the interfacial

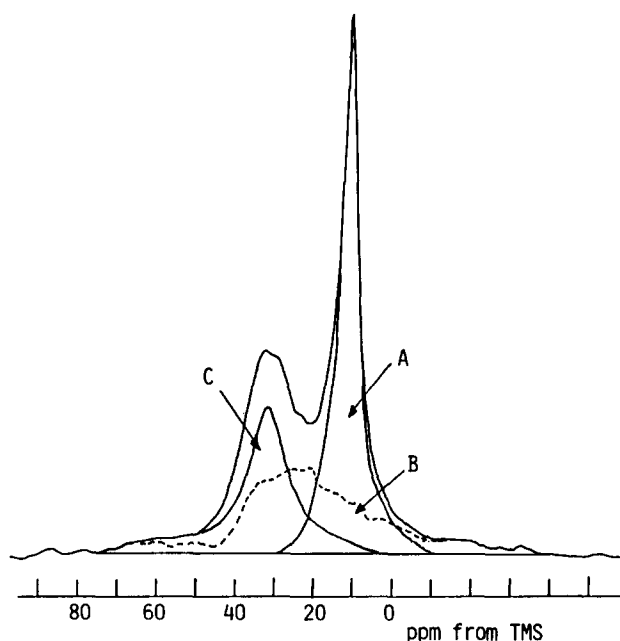


Figure 6 Component analysis of the total spectrum shown in *Figure 2*: A, crystalline; B, interfacial; C, amorphous components. Integrated intensity fraction (%): (a) 50; (b) 29; (c) 21

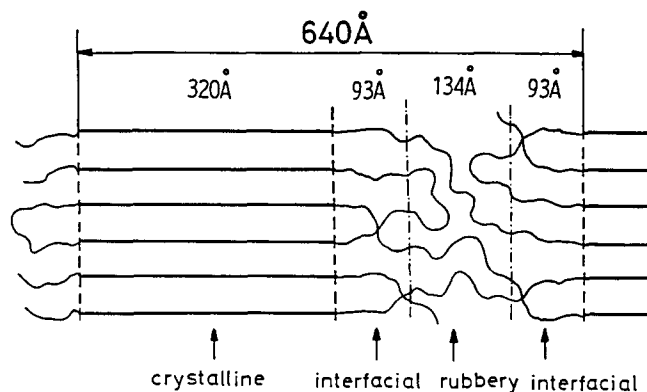


Figure 7 Schematic representation of the phase structure of OPE

region seems to be produced in the fashion expected by the theory. This may be because rapid rearrangement should be possible for the segments in the non-crystalline region during crystallization.

In contrast to isothermal crystallization, crystallization under a uniaxially drawing condition is thought to restrict considerably such rearrangement of the segments in the non-crystalline region. In particular, the segments seem to be limited to exchanging their positions in the lateral direction against the drawing direction. Therefore, structurally irregular parts such as defects or entanglements, which may be mainly expelled from the crystalline region during crystallization, are not readily randomized. This will lead to an increase in thickness for the interfacial region, even if a relatively small amount of the amorphous component appears in the central part of the non-crystalline region as a result of the relaxation of the drawing force in the process of the crystallization.

In such an extremely thick interfacial region of OPE most segments are considerably oriented to the drawing direction, as suggested by the asymmetric n.m.r. lineshape of this component. The lineshape obtained in the rigid state may be described in terms of the superposition of the chemical shift anisotropy for the ^{13}C nuclei with different electronic environments. In principle, the extent of the orientation would be estimated by analysing the lineshape if the effects of the conformation and the molecular packing could be first known. However, it is very difficult at present to determine the lineshape reflecting the chemical shift anisotropy for the rigid carbon with each possible conformation in the non-crystalline region. Furthermore, the molecular motion, which is significantly enhanced at room temperature in polyethylene, makes analysis of the orientation of the segments almost impossible for this sample.

Finally, we should note the contents of the three components with $T_{1\text{C}}=1100$, 60.5 and 5.0 s in the crystalline region. Figures 8a and b show the spectra of the components with $T_{1\text{C}}=1100$ and 60.5 s, respectively, obtained for OPE with the drawing direction perpendicular to the static magnetic field. Here, spectrum (a) was measured by Torchia's pulse sequence with the delay time for the $T_{1\text{C}}$ relaxation set to 300 s. On the other hand, spectrum (b) was obtained by subtracting spectrum (a) from the spectrum measured by the same pulse sequence with a delay time of 30 s. As clearly seen in Figure 8a, the doublet resonance line with equivalent intensities is almost the same spectrum as that expected

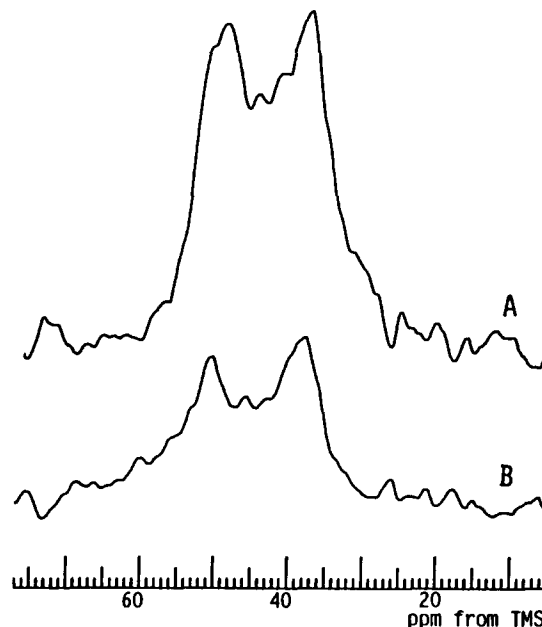


Figure 8 ^{13}C n.m.r. spectra of the crystalline components with A, $T_{1\text{C}}=1000$ s and B, $T_{1\text{C}}=60.5$ s; drawing direction perpendicular to B_0

for the oriented polyethylene crystals⁷ when their chain axis (i.e. the principal axis for σ_{33}) is set perpendicular to the static magnetic field. The chemical shifts of the two peaks are also in good accord with the principal values of σ_{11} and σ_{22} (References 5–8). Therefore, this component is the rigid crystalline component whose chain axis is well oriented parallel to the drawing direction. In contrast, the doublet shown in Figure 8b for the component with $T_{1\text{C}}=60.5$ s is not composed of lines with equal intensities. Such an asymmetric lineshape suggests a broad distribution of the orientation about the drawing direction. Moreover, the shorter $T_{1\text{C}}$ value of this component indicates the onset of the significant local motion in this region. Therefore, this component may be assigned to the slightly disordered crystalline component. On the other hand, the assignment of the shortest $T_{1\text{C}}$ component is not easy at present. However, the $T_{1\text{C}}$ value of 5.0 s is in good accord with the $T_{1\text{C}}$ obtained for the inner CH_2 carbon of n- $\text{C}_{27}\text{H}_{56}$ crystals in the rotating phase¹³. In n-alkanes the rotating phase appears just before melting when the number of carbons is <43 (Reference 14) (or <37 for n-alkanes with high purity¹⁵), and each molecular chain undergoes a rotation about the chain axis in this phase^{13,16,17}. If such small and mobile crystals are included in OPE, they should be located in the disordered region, e.g. on the surface of the crystallites or in the centre of the non-crystalline region. Further discussion of this component will be given after n.m.r. characterization of alkane crystals has been done.

REFERENCES

- 1 Horii, F., Kitamaru, R., Maeda, S., Saika, A. and Terao, T. *Polym. Bull.* 1985, **13**, 179
- 2 Kitamaru, R. and Hyon, S.-H. *J. Polym. Sci. Macromol. Rev.* 1979, **14**, 207
- 3 Kitamaru, R., Horii, F. and Murayama, K. *Macromolecules* 1986, **19**, 636
- 4 Torchia, D. A. *J. Magn. Reson.* 1978, **30**, 613
- 5 VanderHart, D. L. *Macromolecules* 1979, **12**, 1232

Phase structure of oriented polyethylene films: M. Nakagawa et al.

- | | | | |
|----|---|----|--|
| 6 | VanderHart, D. L. <i>J. Chem. Phys.</i> 1976, 64 , 830 | 12 | Yoon, D. Y. and Flory, P. J. <i>Macromolecules</i> 1984, 17 , 868 |
| 7 | Opella, S. J. and Waugh, J. S. <i>J. Chem. Phys.</i> 1977, 66 , 4919 | 13 | Nakagawa, M., Tsuji, H., Horii, F., Kitamaru, R., Takamizawa, K., Urabe, Y. and Ogawa, Y. <i>Polym. Prepr. Jpn.</i> 1988, 37 , 1153 |
| 8 | Earl, W. L. and VanderHart, D. L. <i>Macromolecules</i> 1979, 12 , 762 | 14 | Flory, P. J. and Vrij, A. <i>J. Am. Chem. Soc.</i> 1963, 85 , 3548 |
| 9 | Hama, T., Suzuki, T. and Kosaka, K. <i>Koubunshi Ronbunshu</i> 1975, 32 , 91 | 15 | Takamizawa, K., Urabe, Y., Sasai, S. and Sonoda, T. <i>Polym. Prepr. Jpn.</i> 1987, 36 , 2462 |
| 10 | Chiang, R. and Flory, P. J. <i>J. Am. Chem. Soc.</i> 1961, 83 , 2857 | 16 | Strobl, G. R. <i>J. Polym. Sci. Polym. Symp.</i> 1977, 59 , 121 |
| 11 | Flory, P. J., Yoon, D. Y. and Dill, K. A. <i>Macromolecules</i> 1984, 17 , 862 | 17 | Ewen, B. and Strobl, G. R. <i>Faraday Discuss.</i> 1980, 69 , 1 |